Geology, Geophysics & Environment 2025, vol. 51 (3): 225–242

Variability factors of ^{40}K radionuclide origin in meteorites

Magdalena Długosz-Lisiecka[1], Tadeusz A. Przylibski[2], Katarzyna Łuszczek[3]

[1] *Lodz University of Technology, Faculty of Chemistry, Institute of Applied Radiation Chemistry, Łódź, Poland, e-mail: magdalena.dlugosz@p.lodz.pl (corresponding author), ORCID ID: 0000-0003-1358-049X*
[2] *Wrocław University of Science and Technology, Faculty of Geoengineering, Mining and Geology, Wrocław, Poland, ORCID ID: 0000-0002-8094-7944*
[3] *Wrocław University of Science and Technology, Faculty of Geoengineering, Mining and Geology, Wrocław, Poland, ORCID ID: 0000-0002-2807-4111*

Received: 14 December 2024; accepted: 18 June 2025; first published online: 10 August 2025

Abstract: This study confirms the theory of the variability of the origin of radioactive potassium in various meteorite classes, generated from the dynamic nucleosynthesis (primordial) process, and other processes induced by the solar/cosmic-radiation activation or fractionation caused by the impact vaporization mechanism. High-precision radioactive ^{40}K analysis confirms the differences between various types of meteorites. The concentrations of potassium change from 0.50 ±0.02 Bq/kg (NWA 15015, mesosiderite) to 26.2 ±1.2 Bq/kg (Chelyabinsk, LL chondrite) i.e. three orders of magnitude. All radiometric measurements have been made using a low-background gamma spectrometry system. Additionally, a set of common minerals – Fa (fayalite in olivine), Fs (ferrosilite), and Wo (wollastonite in pyroxenes) – was applied (MetBase n.d.). For the radionuclides factor variability, the principal component analysis (PCA) for the chemometric analysis has been applied. Two factors of the ^{40}K variability have been identified, described, and explained. In this study, PCA was applied for the interpretation of the ^{40}K potassium origin sources in 32 meteorite specimens, represent various groups and classes of meteorites. Two significant PCA factors of variability have been identified, PC1 (51.04%) and PC2 (30.68%), assigned as an activation process by cosmic radiation exposure and a nucleosynthesis mechanism (primordial), respectively.

Keywords: radiation, cosmic rays, nuclei, meteorites, statistics, primordial nucleosynthesis

INTRODUCTION

Potassium is a minor constituent of the Solar System and one of the most common elements of the Earth's crust, where it is exclusively oxyphilic (its content amounts to about 2.41% mass (Palme et al. 2014) or 2.48% mass (Hrynkiewicz 2001)). K is also present as a trace element in the atmosphere and is one of the main cations (K^+) dissolved in seawater (Albarède 2009, Millero 2014). Potassium is classified as a moderately volatile element as its T_c (condensation temperature) is 1006 K (Lodders & Fegley 1998, Lugaro et al. 2018, Lawson et al. 2022, Vasini et al. 2022, Nie et al. 2023a). Melting of the internal structure during planetary differentiation processes, cause the Earth and other differentiated bodies to be depleted of K and other moderately volatile elements by almost one order of magnitude compared to chondrites (Bloom et al. 2020, Nie et al. 2021, Steller et al. 2022). The alkali metal potassium K has three naturally-occurring isotopes: ^{39}K, ^{40}K, and ^{41}K. Two stable isotopes: ^{39}K and ^{41}K, are accounting for 93.2581% and 6.7302% of the total isotopes, respectively. Both isotopes are produced by oxygen burning in massive stellar explosions (e.g., Type II supernovae; Clayton 2003). Radioactive ^{40}K has a long half-life $T_{1/2} = 1.248 \cdot 10^9$ years and its decay products are ^{40}Ca (89.25%) and ^{40}Ar (11.55%) (Zhao et al. 2019). In the whole of the Earth's

structure, ^{40}K reaches 0.0117% of the total K. The average specific activity of the ^{40}K isotope concentration in the terrestrial crust ranges from 258 to 370 Bq/kg; however, the maximum value of 631 Bq/kg and 1850 Bq/kg is reached in basalts, and in granites and syenites, respectively (Atwood 2010). K stable and radioactive isotopes have numerous applications in geochemistry, including surface weathering, hydrothermal alteration, oceanic plate subduction, and global cycling (Li et al. 2019). Potassium isotopes play a significant role in cosmochemistry and have been linked to theories such as the giant impact origin of the Moon or the synestia hypothesis (Hubbard 2016, Lock et al. 2018), solar nebula condensation, planetary formation, and magma ocean evolution. Due to geochemical and cosmochemical properties, the isotopes of K have the potential to be used as tracers for understanding the different evolutionary history of meteorites and the Earth. As a moderately volatile element, K can help us to understand the genetic relations and the thermal history of different groups and subgroups of meteorites and to better explain the mechanisms of the moderately volatile element fractionation during either nebular or planetary condensation/vaporization events (Zhao et al. 2019, Huang et al. 2023).

Potassium is a minor element present in various meteorites, including the iron group. Significant ^{40}K abundance differences have been found between ordinary, enstatite, and carbonaceous chondrites and achondrites, caused not only by the stellar nucleosynthesis process but also fractionation, recrystallisation or cosmic-ray primary and secondary reactions (Rosborough et al. 2019). Thermal processes, nuclear decays, various exposure terms (cosmic ray exposure ages CREAs – different times and particle fluxes in nuclear reactions) present in the history of an individual meteorite matrix generate changes in ^{40}K activity concentration and are the cause of different concentrations of ^{40}K measured in meteorites on Earth (Burnett et al. 1966, Nie et al. 2023b, Voskresensky et al. 2023).

In general meteorite structures, K remains common in lithophilic compounds; however, in iron meteorites, potassium's contribution is in the range from 0.001 to 0.1 ppm. In chondrites, it is present primarily as an admixture in feldspars, while achondrites are poorer in K than chondrites, additionally showing greater concentration fluctuations (13–600 ppm) (Polański 1988). The Moon's rocks (and lunar meteorites) are poorer in K than the terrestrial rocks, and their K/Na ratio is lower (except the KREEP rocks). K also occurs in rocks as a dispersed admixture in pyroxenes or amphiboles, and micas. In sedimentary rocks, K concentrates as evaporite in K and K-Mg chlorides (Polański 1988, Albarède 2009, Kun et al. 2016, Erkaev et al. 2023, Huang et al. 2023, Przylibski et al. 2023, Roland et al. 2024, Varnam et al. 2024).

All meteorites contain the potassium element from mostly two sources. Potassium is formed through nucleosynthesis in massive stars and supernovae, contributing to the interstellar medium from which the solar system originated. This primordial potassium became incorporated into meteorites during the early stages of the formation of solar systems (Fischer et al. 2024). The second source has a spallogenic character resulting from exposure to cosmic rays (induces spallation reactions within meteorites, producing cosmogenic isotopes of potassium). These interactions provide insights into the cosmic-ray exposure histories of meteorites. Additionally, redistribution of ^{40}K isotope is possible and concentration of isotope can be controlled by thermal processes which parent body underwent (magmatic differentiation, post magmatic, i.e., pneumatolytic processes, and metamorphic processes, i.e., metasomatic exchanges). The celestial bodies of the Solar System are routinely exposed to cosmic radiation, mostly high-energy particles which initiate nuclear reactions on the material and as result produce radioactive isotopes (Goriely & Pinedo 2015, Curry et al. 2022, Frizzell et al. 2023, Nie et al. 2023b, Dauphas et al. 2024).

Several studies use the ^{40}K/K ratio as a common method for meteorite age determination (Ku & Jacobsen 2020). In comparison with different methods based on shorter-lived radionuclides, e.g., ^{26}Al/^{21}Ne or ^{36}Cl/^{36}Ar and ^{39}Ar/^{38}Ar, this method yields results about 35–50% higher (Hampel & Schaeffer 1979) or 40% lower in comparison to ^{3}He, ^{21}Ne, and ^{38}Ar dating methods (Ammon et al. 2009). Hampel and Schaeffer (1979) indicate that the difference between dating results is probably caused by variations in cosmic ray intensity in the

inner Solar System. Burnett et al. (1966) indicate that the differentiation of the isotopic composition of potassium occurs in two cases, i.e., due to a various chemical composition and size distribution, in both parent and meteoroid bodies. The abundance of the element in iron meteorites is low and does not exceed 0.1 ppm. The initial ^{39}K,^{40}K, and ^{41}K isotope contents in celestial bodies depend on the composition of interstellar clouds. Several studies have confirmed that meteoritical potassium is a mixture of cosmogenic and 'primordial' potassium (from the nucleosynthesis process) (Ammon et al. 2009, Tian et al. 2019, Zhao et al. 2019, Nie et al. 2023a). However, for planetary objects with a primordial crust such as the Moon, K depletion may be due to the loss of K as the primordial crust cooled from a magma ocean (Taylor & McLennan 2010, Jaumann et al. 2012, Mayer 2012, Barr 2016).

Herzog (2007) confirmed that primordial potassium in stony meteorites exceeds the contribution of the spallogenic component (Nie et al. 2023b). Iron and stony iron meteorites contain measurable potassium abundances even for a relatively short cosmic ray exposures time (i.e., 10 Myr). The meteorite evolution and its exposure history (π(plane) or 2π(sphere)), in theory can be described by the one-stage irradiation model of the meteorite bulk. In a parent body structure, the internal material, located many meters under the surface, has been shielded from cosmic rays. As a result of collisions, a fragment can be excavated and pushed out freely as a liberated meteoroid. The new object becomes fully exposed to cosmic rays (2π), orbits the Sun, until it finally strikes the Earth. The cosmic ray exposure age (CREA) and radiation flux have a significant influence on the component deconvolution to distinguish radiogenic, trapped and cosmogenic components in the isotope signature. Therefore, radioactive isotope composition, measured during the last few half-lives of nuclides, can supply valuable information about the age of the exposure (CREAs), different parent bodies origin and shielding depth, preatmospheric radius of the meteoroid, exposure history (one of two steps), terrestrial age, crystallization age, etc. (Herzog 2007).

Establishing and interpreting the ^{40}K isotope abundances is challenging for a number of reasons. The ^{40}K isotope production is a function of various processes, it can occur either in various stellar processes with a low efficiency (e.g., oxygen burning in massive stellar explosions; Clayton 2003) or different nuclear reactions, based on a cosmic-ray-induced spallation on the main target elements like Fe or Ni or slow neutron-capture processes (Goriely & Pinedo 2015). The mixing of different components during thermal processes in the solar nebula is an unlikely explanation for the overall K isotope variations found in chondrites (Ku & Jacobsen 2020). However, a later study has shown that ^{41}K/^{39}K isotopic variations in carbonaceous chondrites are due to mixing between different chondritic components (Nie et al. 2021) while in contrast ^{40}K in meteorites reflects both nucleosynthetic and cosmic ray induced anomalies (Nie et al. 2023a).

Enrichment of the ^{50}V, ^{40}Ca, ^{43}Ca, and ^{40}K isotopes due to cosmic radiation has been noticed by Stauffer and Honda (1994) in Aroos (officially classified as a Yardymly IAB complex iron meteorite, found in 1959 in Azerbaijan) and in other iron meteorites. The enrichment of these isotopes may prove their common origin as spallation products from high-energy nuclear reactions with the Fe fraction. Stable isotopes of potassium, ^{39}K and ^{41}K, in iron meteorites were produced by spallation reactions (Wang et al. 2021). In 2004, Napolitani and co-workers estimated cross sections for ^{39}K, ^{40}K, and ^{41}K reaction based on spallation injected by protons equal to 8.06 ±0.88 mb, 13.68 ±1.47 mb, and 10.22 ±1.11 mb, respectively. These data favour the ^{40}K production and change the isotopic composition in comparison with terrestrial composition, resulting from a nucleosynthesis process in the past. In practice, in old (long duration spallation process in space, high CREAs) iron meteorites, cosmogenic ^{40}K component exceeds the natural (radioactive) ^{40}K content. In stony meteoroids, the native potassium exceeds the cosmogenic component due to the shorter age of meteorites (lower CREAs, shorter exposure duration), lower iron concentration, smaller size, and different nuclear reaction channels for other chemical components of meteorites.

Additional ^{40}K could have been produced by capture in stable ^{39}K of neutrons from irradiation. In this theory, in the terrestrial matter, some

contribution of ^{40}K comes from a cosmogenic source (David & Leya 2019, Li et al. 2019).

Gastis et al. (2020) noticed the nuclear reactions which determine the production of ^{40}K during stellar evolution may perform a critical role. Zhao et al. (2019) confirmed that enstatite chondrites display significant ^{41}K/^{39}K variations, without definitive trends among the chemical groups (EH and EL chondrites), petrological types (3–6), shock degrees (S2–S4), and terrestrial weathering conditions. Ku and Jacobsen (2020) indicated the correlation of K with other neutron-rich nuclides, ^{64}Ni and ^{54}Cr. They concluded that the K isotope anomalies are inherited from an isotopically heterogeneous protosolar molecular cloud with a limited radial mixing in the protoplanetary disk. The thermal processing in the solar nebula results in the depletion of the solar system bodies in moderately volatile elements, fractionation, and the evaporation effect. Gastis et al. (2020) added an astrophysical reaction rate of ^{40}K(n, p)^{40}Ar responsible for the decreasing of ^{40}K content during stellar nucleosynthesis.

Primary (mostly protons) and secondary (neutrons) cosmic-rays induce a large variety of high- and low-energy nuclear reactions. GCRs mostly take place in high energy nuclear reactions, with the domination of spallation reactions. The secondary cosmic-ray particles, especially the neutrons, primarily account for low energy reactions (<100 MeV), where the epithermal and thermal neutron capture processes dominate. The primary and secondary radiation and energy distribution of the particles influence the nuclear reaction channel and final isotope composition. As a result, the isotope production rate is proportional to the cross section of the production of specific nuclides. The half-life of ^{40}K is too long to reach saturation level in (any) typical meteoroids. The high density and large size of many iron and stony meteorites generates a shielding effect (Flynn et al. 2018).

The aim of this study is to supplement knowledge on the range of the ^{40}K concentration in various types of meteorites on the basis of our own low-background measurements. The secondary goal of our work is to verify the origins of the ^{40}K isotope in different groups of meteorites by applying PCA analysis. Principal component analysis (PCA) is a dimensionality reduction and machine learning method that enables the simplification of a large data set into a smaller set, while preserving significant patterns and trends. It achieves this by transforming the original correlated variables into a new set of uncorrelated variables called principal components. In the context of geochemical or isotopic analyses (e.g., K-40 in meteorites), PCA can help reveal underlying factors driving variability, such as cosmic exposure history, mineralogical differences, or potential terrestrial contamination. It also allows us to quantify the contribution of each factor to the total variance.

In this research, PCA is used to identify the factors determining the concentration of the K isotope in the material, and in relation to samples of meteorites of different origins, it was applied to determine quantitative trends. Essentially, the analysis aims to help answer the question of where the ^{40}K in meteorites comes from and what processes conditioned the accumulation or reduction of this isotope. Additionally, the second isotope ^{26}Al, was used in this study as a safeguard to facilitate the definition of factors identified by the PCA. Both isotopes – ^{26}Al and ^{40}K are correlated when the most important factor in their genesis is production by the influence of cosmic radiation. The ^{26}Al produced during nucleosynthesis has already completely decayed, therefore the high values of the correlation coefficient between the content of both isotopes indicate the paramount importance of cosmic radiation in the production of ^{40}K present in the meteorite, which depends on its CREA.

Review of ^{40}K isotope nuclear production channels

Possible nuclear production channels for cosmogenic ^{40}K in meteorites have been investigated. For this research, the open EXFOR Experimental Nuclear Reaction Data (IAEA) base has been applied (Fig. 1 on the interleaf) (EXFOR (IAEA) n.d., Otuka et al. 2014, Zerkin & Pritychenko 2018). Five nuclear reactions have been identified as possible channels for this isotope production as a result of the interaction between a cosmic ray and the structure of a meteorite parent body. In general, an increase of duration of a parent body exposure to the cosmic radiation causes an increase of cosmogenic ^{40}K content.

Both SCRs and GCRs initialize two types of nuclear reactions based on cosmic-ray-induced spallation by high energy primary particles on Fe or Ni nuclei; nuclear activation reactions e.g., ^{40}Ar(p, n)^{40}K or neutron capture reactions by secondary thermal neutrons.

Figure 1 compiles five different sets of plots for various nuclear reactions as some examples, based on results downloaded from the EXFOR database. Figure 1A depicts the channel of interaction of high-energy protons with Fe (all isotopes in natural abundances). The plot represents the dependence of the cross-section (barn) on the energy of the so-called 'projectile' particle on the target material in ^{40}K production. Figure 1B represents results of ^{39}K(n, γ)^{40}K reaction channel, however energy of particles is much lower (achievable data). Figure 1C represents results of ^{39}K(n, γ)^{40}K reaction.

An increase of potassium isotope productions in meteorites is caused by thermal neutron capture reaction ^{39}K(n, γ)^{40}K, but also by nuclear activation, e.g., ^{40}Ca(n, p)^{40}K shown in Figure 1D, ^{41}K(n, x)^{40}K, visible in Figure 1E. A slow neutron-capture process (s-process) via the ^{39}K (n, γ)^{40}K re action and oxygen burning in massive stellar explosions are two potassium isotope ^{40}K production channels of stellar nucleosynthetic processes (Clayton 2003).

Zao et al. (2020) noticed that a cosmogenic production of the K isotopes from Fe should be most noticeable in samples with high Fe contents due to more target nuclei and proton activation. Several studies confirm the production of all isotopes of K, including ^{40}K in iron meteorites (Voshage et al. 1983) and stony meteorites (Herzog et al. 2009, Voskresensky et al. 2023).

In practice, various stony meteorites including HEDs, aubrites, lunar meteorites, carbonaceous and ordinary chondrites, as well as stony-iron and iron meteorites contain different ^{40}K concentrations, further validating their formation in different regions of the solar nebula or planetary-like environment (differentiated objects like the Moon or the Vesta asteroid), and in diverse cosmic-ray exposure age (CREAs).

Fractionation of the elements

The concentration of K can be influenced by evaporation under Rayleigh–Taylor conditions as the cause of depletion of moderately volatile elements. Potassium is known as a moderately volatile element (50% T_c of 1006 K) (Lodders & Fegley 1998). Therefore, several works revealed the variations in the K isotopic compositions between different planetary materials (Zhao et al. 2019, Wang et al. 2021).

Potassium as an element tends to quantitatively enter melts during partial melting processes, evaporation, or condensation fractionation mechanisms.

In Bloom's work (2020), there were two possible confirmed scenarios for the explanation of these phenomena:

1) a process occurring in the solar nebula environment:
   - incomplete condensation in the early Solar System (Ciesla 2008);
   - partial evaporation of interstellar dusts (Yin 2005) in the solar nebula (Huss et al. 2003, Huss 2004);
   - mixing of chondrite components formed in distinct volatile-rich and volatile-poor reservoirs (e.g., Alexander et al. 2001);
2) planetesimal creation mechanism including:
   - accretional volatile loss (Albarede 2009, Hin et al. 2017);
   - giant impacts (Paniello et al. 2012);
   - magma ocean degassing (Kato et al. 2015);
   - extraction into atmospheres and atmospheric losses (Fegley et al. 2016).

As a result of some of these processes, it is possible to observe the depletions of volatile elements among various meteorites. Bloom et al. (2020) explained the K isotope fractionation observed in the carbonaceous chondrites with a combination of both nebular and parent-body processes.

MATERIAL AND METHODS

We conducted a multidisciplinary study of several meteorites representing various groups and classes. To obtain contributions from each process, two radionuclides ^{26}Al and ^{40}K concentrations and major minerals composition were measured in all known chondrite groups (ordinary, enstatite, carbonaceous) and achondrite meteorites (iron meteorites, ureilites, eucrites, mesosiderites, pallasites, lunar, and HED) specimens. To estimate the contributions of radioactive potassium from various sources in meteorites, chemometric methods were

applied. An analysis of the results estimates a primordial and spallogenic potassium component.

In order to identify the sources of variability of the potassium ^{40}K isotope, the method of principal components analysis (PCA) was applied. This is used to reduce the number of variables describing the occurrence of a given phenomenon and to find regularities between the variables. In this research, Kaiser's criterion for the selection of the number of significant components and the Varimax rotation method were applied, which is typically used for factors that are potentially independent of each other. Results were analysed in a spreadsheet and the following plots of the sources of the variability were obtained. The test was repeated several times in different configurations due to the smaller influence of some factors (a low content of wollastonite in individual samples). PCA was applied to the database, built including a radiometric approach (two long-lived radionuclides, ^{40}K and ^{26}Al) and three common mineral phases: fayalite (Fe-olivine), ferrosilite (Fe-orthopyroxene), and wollastonite.

The anomalies in the concentration of the ^{40}K isotope in different groups of chondrites and achondrites should be investigated. The ^{40}K and ^{26}Al contents were tested with a low background gamma spectrometer in 29 meteorites, 38 specimens in total, including various groups, petrographic types, weathering grades, shock stages, and both finds and falls of meteorites (Fig. 2).

Most meteorite specimens come from the collection of the Geological Museum of University of Lodz. Only HaH 346 (10 samples) come from two different sources (two different groups of meteorite hunters): seven items from a commercial collection and three items from a private collection. The selection of specimens and their groups was dictated by the available resources. All samples were on loan for the duration of the radiometric analysis. Long term measurements lasting over one year in total were carried out in the Lodz University of Technology in the Institute of Applied Radiation Chemistry, precisely the Laboratory of Isotopic Methods. In this study, a unique, low-background (with active and passive reduction of the background) gamma spectrometry system has been applied (Długosz-Lisiecka 2016, 2017, 2019, 2022). The applied method was non-destructive for the samples. The detection efficiency for the whole specimens was determined by the LabSOCS method for the quantitative analysis of the specimens. Each sample measurement was carried out over 320,000 s to reduce the uncertainty of the both isotopes activity concentration analysis (Długosz-Lisiecka et al. 2022).

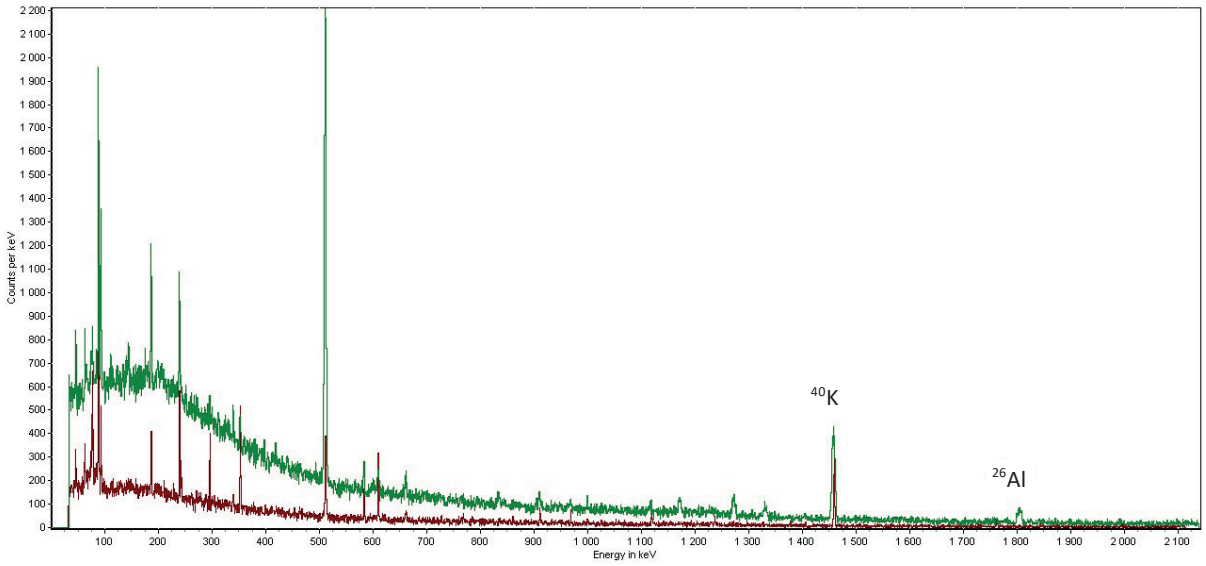

Fig. 2. *Spectrum of the OC meteorite specimen (green line), background (brown line). ^{40}K (1460.8 keV peak energy line) and ^{26}Al (1808.7 keV peak energy line)*

In the radioanalytical approach, only long-lived radionuclides, ^{40}K, $T_{1/2} = 1.248 \cdot 10^9$ years and ^{26}Al, $T_{1/2} = 7.17 \cdot 10^5$ years were analysed based on the 1460 keV and 1808 keV peak energy line, respectively (NDS Nuclear Data Services (IAEA) n.d.).

Several well-known specimens of meteorites, representing various classes and groups, were analysed. The authors used meteorite samples from 7 observed falls and 22 finds (Table 1). For the HaH 346 chondrite, the ^{40}K isotope abundances have been analysed in 10 different specimens independently to test homogeneity of this meteorite by repeated measurements. The samples of the same chondritic meteorites have been used to check the homogeneity of the samples and robustness of the measurements of the ^{40}K isotope.

In most cases, the analysed chondrites were the higher petrographic types of 5 or 6 and had different shock stages (S1–S4). Those from observed falls had low weathering changes (W0), while the others (finds) had a higher weathering grade (W1–W4).

Table 1
List of meteorites (characterized after the MBD Meteoritical Bulletin Database n.d.), specimens of which were examined for the ^{40}K and ^{26}Al activities concentration

No.	Meteorite name	Class, group, subgroup*	Applied mass [g]	Fall/find location, Year of find/fall
1.	Northwest Africa 8529 (NWA 8529)	OC, H6, S2, W2	84	Northwest Africa, 2014 (found)
2.	Sayh al Uhaymir 542 (SaU 542)	OC, H6, S1, W3/4	65	Al Wusta, Oman, 2011 (found)
3.	Tamdakht	OC, H5, S3, W0	60	Tamdakht (Ouarzazate), Morocco, 2008 (fall)
4.	Chergach	OC, H5, S3, W0	105	SW El Mokhtar, Erg Chech, Timbuktu district, Mali 2007 (fall)
5.	Gao-Guenie	OC, H5	54	Gao, a village about 60 km N of the town of Leo, Upper Volta, Burkina Faso 1960 (fall)
6.	Pultusk	OC, H5	280	Poland, Ostrołęka, 1868 (fall)
7.	Buzzard Coulee	OC, H4, S2, W0	56	Wilton Rural Municipality, Saskatchewan, Canada, 2008 (fall)
8.	Ghubara	OC, L5	104	Oman, 1954 (found)
9.	Sayh al Uhaymir 001 (SaU 001)	OC, L5, S2 W1	87	Oman, 2000 (found)
10.	Hammadah al Hamra 346 (HaH 346)	OC, L6, S5, W0	134 221 198 201 200 207 163 120 141 54	Gharyan, Libya, 2019 (found)
11.	Aba Panu	OC, L3, S4, W0	154	Oyo, Nigeria, 2018 (fall)
12.	Chelyabinsk	OC, LL5, S4,W0	78	Chelyabinskaya oblast', Russia, 2013 (fall)

Table 1 *cont.*

No.	Meteorite name	Class, group, subgroup*	Applied mass [g]	Fall/find location, Year of find/fall
13.	Northwest Africa 4561 (NWA 4561)	EL-melt rock	90	Erfoud, Morocco, 2006 (found)
14.	Allende	CV3	48	Chihuahua, Mexico, 1969 (fall)
15.	Northwest Africa 14149 (NWA 14149)	CK4	164	Northwest Africa, 2021 (found)
16.	Northwest Africa 8095 (NWA 8095)	CO3, S1, low	31	Northwest Africa, 2013 (found)
17.	Gibeon	Iron, IVA	33	Namaland, Namibia, 1836 (found)
18.	Odessa	Iron, IAB-MG	37	Texas, USA, 1922 (found)
19.	Morasko	Iron, IAB-MG	379	Poland, 1914 (found)
20.	Northwest Africa 11421 (NWA 11421)	Lunar (feldspathic breccia)	5.2	Northwest Africa, 2017 (found)
21.	Northwest Africa 15604 (NWA 15604)	Lunar (feldspathic breccia)	40	Northwest Africa, 2022 (found)
22.	Seymchan	Pallasite, PMG	23	Magadanskaya oblast', Russia, 1967 (found)
23.	Northwest Africa 10505 (NWA 10505)	Diogenite, HED achondrites	26	Northwest Africa, 2015 (found)
24.	Northwest Africa 6069 (NWA 6069)	Ureilite	28	Northwest Africa, 2009 (found)
25.	Northwest Africa 2698 (NWA 2698)	Howardite, HED achondrites, S3-5, W2	12	Northwest Africa, 2004 (found)
26.	Northwest Africa 6266 (NWA 6266)	Mesosiderite-B4	8	Northwest Africa, 2010 (found)
27.	Northwest Africa 15015 (NWA 15015)	Mesosiderite	331	Northwest Africa, 2022 (found)
28.	Camel Donga	Eucrite-mmict, HED achondrites	15	Western Australia, Australia, 1984 (found)
29.	Djoua 001	Aubrite	101	Algieria, 2021 (found)

* For ordinary chondrites (OC) the information on shock stage and weathering grade is included.

RESULTS AND DISCUSSION

There are several possible nuclear reaction channels for the production of the ^{40}K nuclide by cosmic rays, based on protons (primary cosmic radiation) or thermal/epithermal neutron (secondary cosmic radiation) capture. Results of the ^{40}K isotope concentrations presented in the literature in meteorite samples fluctuate in a wide range, from 280 ±50 dpm/kg (dpm – disintegrations per minute) (Povinec et al. 2015) to 2000 ±150 dpm/kg (Povinec et al. 2020). In this study, the ^{40}K activity concentration changed from 21.9 ±0.5 dpm/kg to 2661 ±90 dpm/kg in various meteorite specimens. The results of all measurements of the ^{40}K activity concentration in the studied meteorites are presented in Figures 3 and 4. The highest value of the ^{40}K activity concentration equal to 26.2 ±1.2 Bq/kg was found in the Chelyabinsk (LL chondrite) and only a slightly lower value (25.7 ±1.1 Bq/kg) in the ordinary chondrite of the (L chondrite) – NWA 14149. However, the lowest values of ^{40}K activity concentration were measured in the NWA 15015 (mesosiderite) 0.50 ±0.02 Bq/kg.

In the case of the K isotope fractionation (in different meteorites), the abundance of ^{40}K will potentially change. This can be the result of the primordial and cosmogenic (secondary) origin of ^{40}K. The clear cosmogenic character of ^{40}K is shown in Figure 3, where the potassium radioactive isotope occurs in a specific correlation with the ^{26}Al isotope.

In theory, cosmogenic ^{40}K can be a product of the nuclear reaction of the cosmogenic radiation to Fe present in meteorites (Fe(total isotopic content) $(p, x)^{40}$K, with a cross section equal to 8 ±1 mb for energy 0.73 GeV of protons). Alternatively, an order of magnitude more effectively, cosmogenic ^{40}K isotope production can be allowed by a low-energy neutron capture by the stable isotope ^{39}K, e.g., in reaction ^{39}K$(n, g)^{40}$K with a cross section equal to over 8.8 b (Guber et al. 2007). The occurrence of probable reactions as a result of which the ^{40}K isotope can be produced in meteorites generates a strong theoretical basis for the prediction of its cosmogenic contribution.

In the stony meteorite specimens, the major amount of the ^{40}K activity has a primordial origin (Fig. 4). In each meteorite class, its concentration can vary widely, due to other processes like cosmic exposure, thermal history and group. The cosmogenic contribution depends on its chemical composition, especially the content of Fe, Ca, Ar, and K stable isotopes, type of particles initialized by protons or neutrons, and its energy. Due to the high density and shielding character of the meteoroid matrix, particle flux can change, and reaction channels can be more efficient (for neutrons) or less efficient (for protons). The occurrence of a different meteorite chemical or mineral composition (silicates and metal phases) can locally change the ^{40}K production (Marshall 1962, 1968, Bogard et al. 1967).

Several studies describing Antarctic finds have shown that the K isotopic composition of Antarctic meteorites has not been altered compared to meteorite falls. However, one detailed study has observed substantial K enrichment in hot desert meteorites and attributed this to terrestrial alteration, probably from the precipitation of K-bearing salts and sulphates (e.g., sylvite (KCl)) and confirmed a large range of K isotopic compositions (including ^{40}K) for meteorites even from the same fall (Zhao et al. 2019).

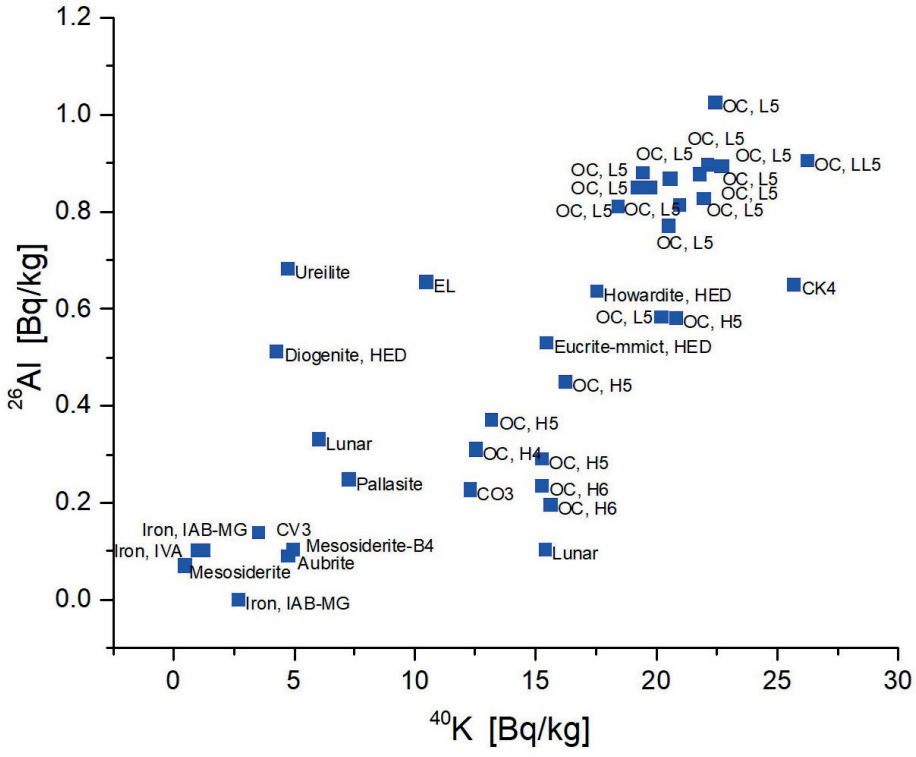

Fig. 3. *^{40}K and ^{26}Al activity concentration correlations in various meteorites*

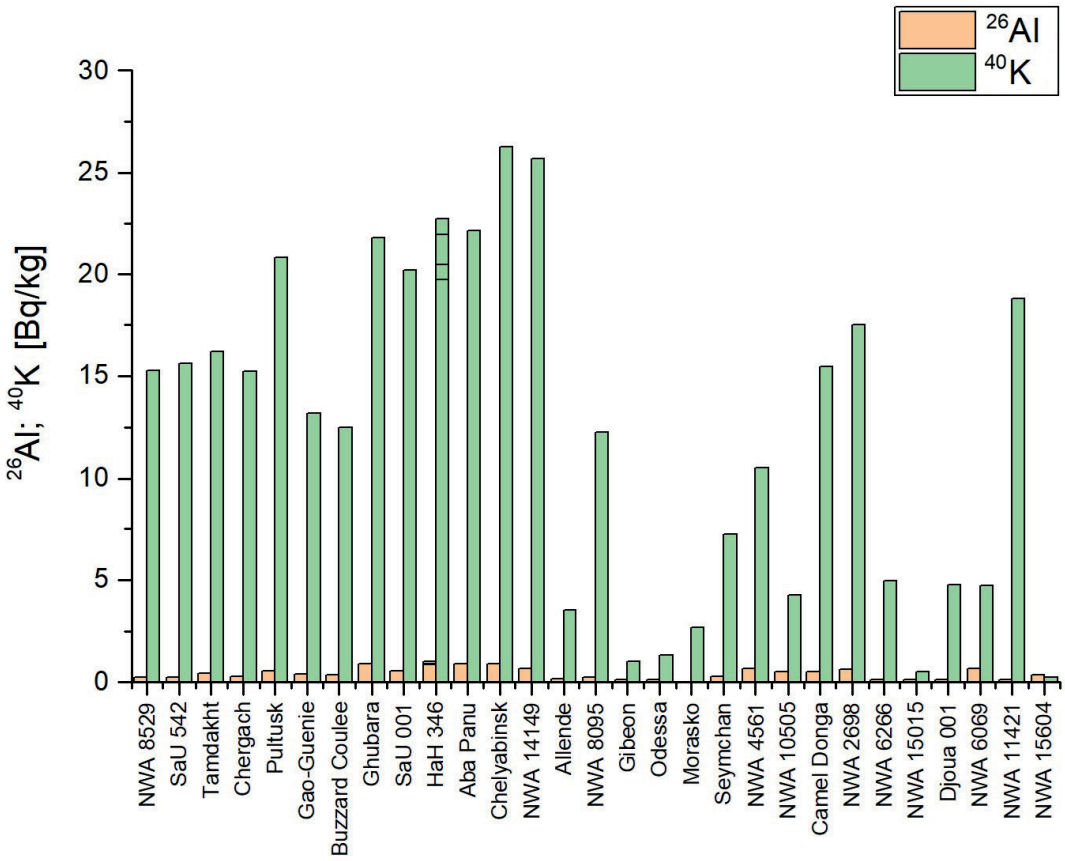

Fig. 4. *^{40}K and ^{26}Al isotopes activity concentrations*

On the other hand, ^{40}K isotope activities can change with density, chemical composition, and pre-atmospheric radius of the meteoroid.

For this reason, the percentage content of three minerals one from the group of olivines (fayalite, an iron-rich end member of the olivine isomorphous solid solution series), and two of pyroxenes (ferrosilite, an iron-rich end member of the orthopyroxene solid solution series and wollastonite, the calcium end member of the pyroxenoids), commonly found in the studied meteorites, was obtained from the literature (Saunier et al. 2010, Korda et al. 2023) (Fig. 5).

Five variables were used for the analysis: the concentration of the isotopes ^{40}K and ^{26}Al (Fig. 3), and the contents of Fa, Fs, Wo (Fig. 4). The PCA analysis reduces the number of variables and creates new non-physical variables in the form of principal factors. Usually, the main factors that explain the total variance to the greatest extent are considered (criterion >10% was used). Two main factors PC1 and PC2 (with eigenvalue >1) explain about 82% of the total variance (Table 2).

Table 2
Summary of the PCA analysis factors

No.	Eigenvalue	Percentage of explained variance [%]	Cumulative value [%]
1.	2.55	51.04	51.04
2.	1.53	30.68	81.73

The cumulative percentage of the explained variance of the analysed variables (Table 2) was defined as the smallest number of principal components for which the sum of their variance's accounts for a certain portion of the variance of all the variables subjected to reduction.

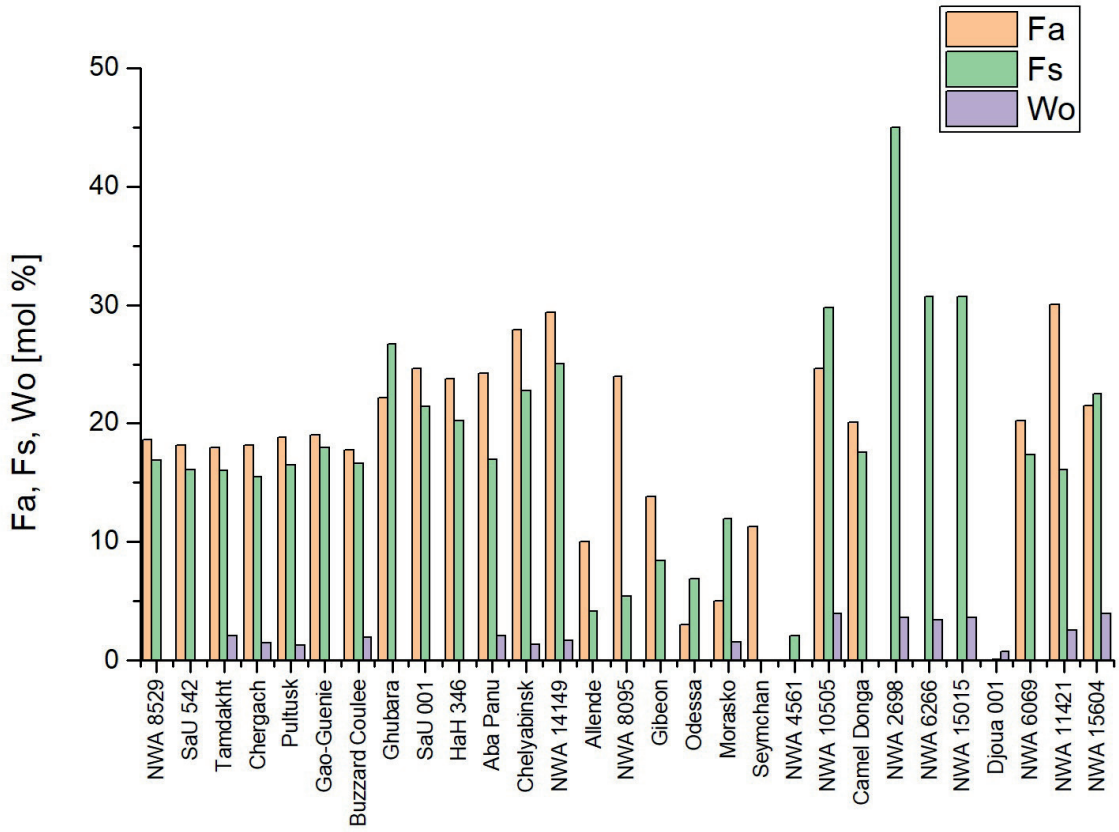

Fig. 5. *Fa, Fs, and Wo in meteorites (MBD Meteoritical Bulletin Database n.d.)*

According to various sources, the lower limit that this sum must exceed is 75%. In this study we applied Kaiser's criterion and considered principal components with eigenvalues greater than one (alternatively, the percentage of the explained variance must be greater than 10%).

A detailed summary of the main factors is shown in Table 3. This table directly indicates the impact of the input data, i.e., ^{40}K, ^{26}Al or Fa, Fs, Wo, on the results of the PCA analysis, i.e., new variables in the form of the main factors. PCA allows for determining whether there is a set of latent features that generate the observed ^{40}K concentrations. All of the values presented in Table 3 are vectors.

Table 3 shows principal component factors for all the analysed variables. The most significant component (PC1) highly corresponds to the ^{40}K, ^{26}Al isotopes and Fa (fayalite in olivines) contribution. Component no. 2 (PC2) corresponds to the Fs and Wo contributions, i.e. with pyroxene minerals.

Table 3
Influence of the input data on the PCA factors (bold values are statistically significant)

Variables	Principal component PC1	Principal component PC2
^{40}K	0.58	0.00
^{26}Al	0.56	0.03
Fs	0.23	0.71
Fa	0.51	−0.05
Wo	−0.21	0.71

The PC1 (percentage of explained variance equal to 51.04%) factor appears to be an activation process – generating ^{40}K in the meteoroid (Fig. 6). It should be emphasized that activation is a process that is quantitatively dependent on several factors:

the number of target atoms (potentially Fe, Ar in direct reactions with protons, or the ^{40}Ca or ^{39}K isotopes in the secondary reactions with neutrons). The PC1 factor is particularly important for the content of the ^{40}K isotope in the lunar meteorite. The Moon, made of feldspar (the main mineral of anorthosites) and basalt, relatively younger than other studied meteorites, has favourable conditions for the accumulation of the ^{40}K isotope from several reaction channels due to the distance to the Sun and a higher solar radiation dose rate (Eugster et al. 2006).

Figure 7 directly shows the value of the identified components for each meteorite specimen. The principal component analysis indicates variation factors showed that the first factor of variation is responsible for about 51%, the second factor for about 30%, and the third factor for about 10% of the variability of the observed results (not statistically significant, according to Kaiser's criterion).

The production of ^{40}K can not only occur through the (*p*, *x*) reaction, (e.g., Fe) but also competitively through (*n*, *x*) reactions, where the reaction channel on ^{40}Ca is the most favoured (Fig. 1D). Therefore, the greatest ^{40}K activities are observed in those meteorites that naturally contain silicates in the form of both olivines and pyroxenes. A good example is the LL chondrite Chelyabinsk, where the highest activity of the isotope was observed. Lower contents of potassium ^{40}K are observed in specimens containing a high content of Fe. The PC1 factor clearly correlates potassium ^{40}K with the elemental composition of measured sample, which confirms the presence of the oldest silicate material constituting the chondrules and matrix of chondrites. The positive value of the PC1 factor (Fig. 8) presumably indicates the current presence of the ^{40}K isotope in the chondrites. Negative values, on the other hand, may indicate the absence of the ^{40}K isotope of a primary origin which means that the ^{40}K activity deposited in the silicate material of chondrites could have undergone natural decay or a reduction in the mass of silicate material during subsequent processes, e.g. fractional melting and crystallization. The silicate material that builds the parent bodies of chondrites, about 4.5 billion years old, may have lost a significant portion of the activity of this isotope, considering its decay time of about 1.25 billion years.

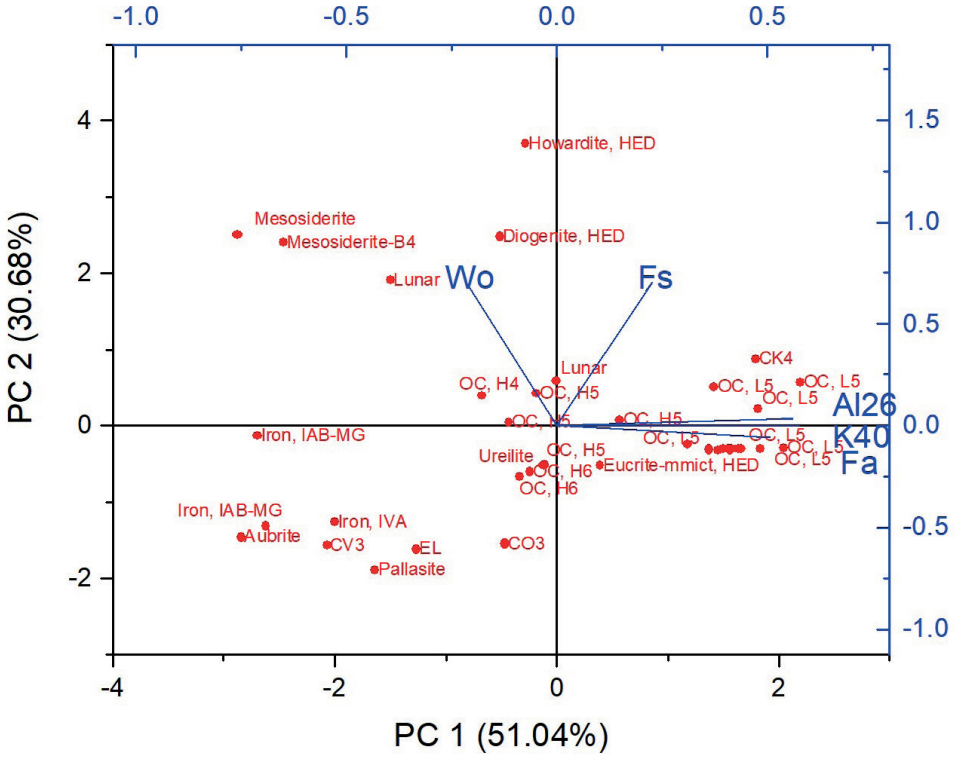

Fig. 6. *Correlation of PC2 (30.68%) and PC1 (51.04%) components in various meteorites*

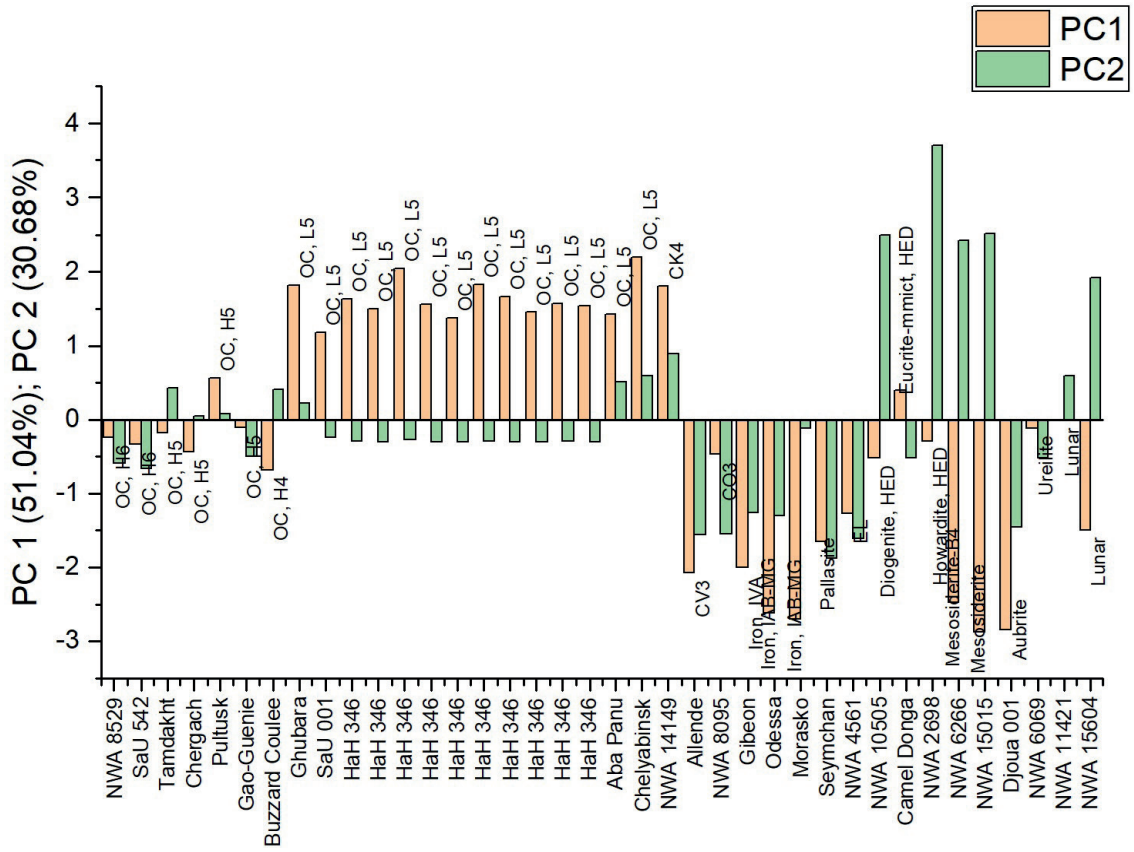

Fig. 7. *Identified two PC1 and PC2 components of variability, compiled for individual groups of meteorites*

As Table 3 indicates, ^{40}K has no effect on the PC2 factor (vector equal to 0.00), so it appears that PC2 may be the component that corresponds to the nucleosynthetic process that, in general, determined the isotopic composition of elements 4.5 billion years ago and determined the ^{40}K content of objects in the Solar System. The decay time of ^{40}K is about 1.25 billion years, so after 4.5 billion years, only 8.2% portion of original nucleus of potassium from nucleosynthesis remains. We can presume that one of the factors connecting all of the samples is the effect related to the mechanism of the primary potassium synthesis (nucleosynthesis – in stellar nebulae or in the core) (Bloom et al. 2020, Ku & Jacobsen 2020, Nie et al. 2023b). This factor is significantly related to chemical composition and will clearly differentiate individual groups of meteorites, depending on their structure and origin (Hu et al. 2024).

After identifying the main factors of ^{40}K variability using factor analysis, an additional statistical tool such as multiple regression can be used to assess the predicted concentration of ^{40}K. This simple statistical approach can even be used in MS Excel in the data analysis section. The difference between the measured and predicted concentrations defines the residual.

Figure 8 shows the predicted portions of the ^{40}K content in various meteorites. In some specimens like NWA 6069 (ureilite) or NWA 10505 (diogenite), the abundance of the isotopic potassium was overestimated. The measured values were significantly lower than those predicted by the PCA analysis. The reasons for such a disproportion are possibly other processes which define the isotopic signatures and a unique mineral composition, especially linked with the parent body structure and composition.

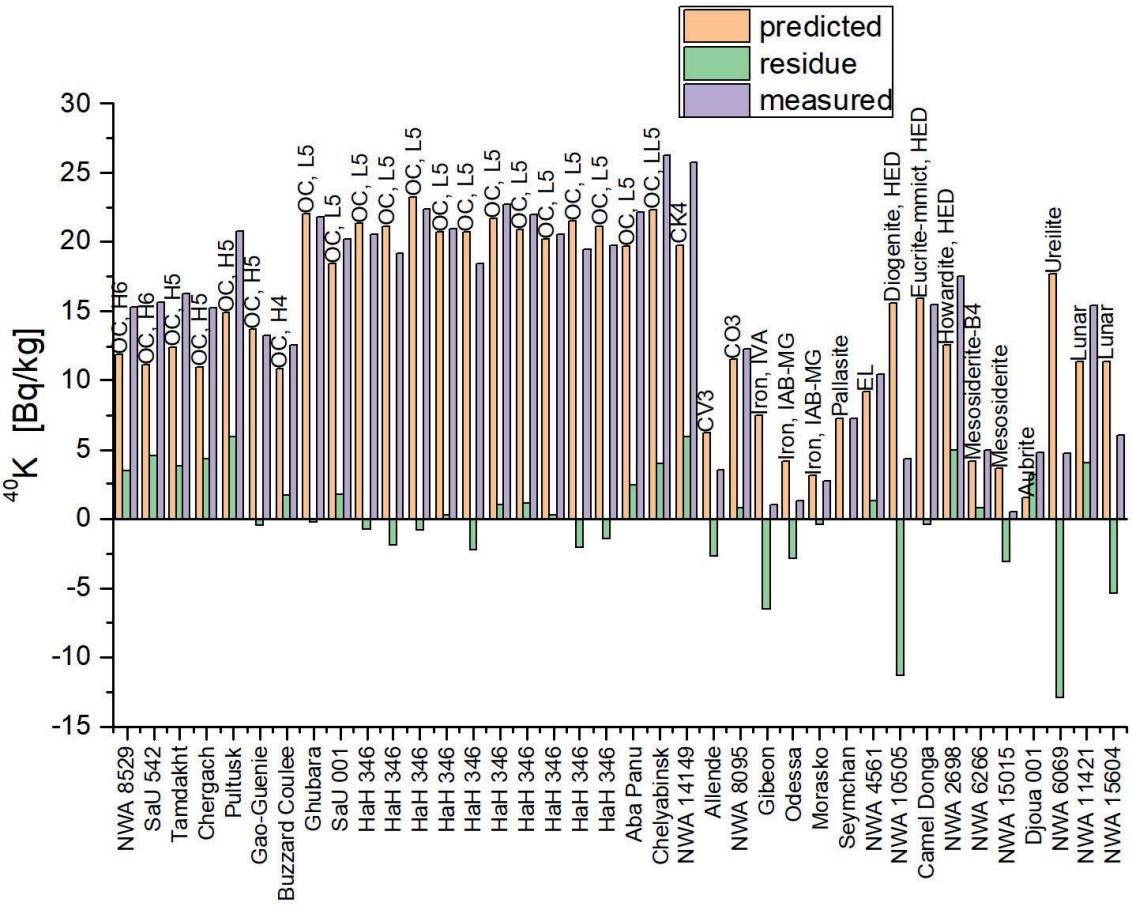

Fig. 8. *Measured, predicted, and undefined residue of the ^{40}K activity in the measured meteorite specimen, based on multiple regression*

DISCUSSION

Determination of the ^{40}K isotope production dynamic is a simple function, but its application is only possible when the exposure age of meteorites is well known. In practice, the excess of the ^{40}K isotope resulting from a different cosmic exposure age causes the variability of potassium concentrations even in the same meteorite group and class. Moreover, impact events cause the degassing of parent rocks and resetting of isotopic signature (e.g., Ar-Ar) and consequently a lower amount of radiogenic ^{40}K from ^{40}Ar decay. Advanced analytical methods like PCA are essential to unravel the complex history and behaviour of potassium in extraterrestrial contexts. The principal component PC1 (51.04%) is the axis that explains the largest portion of the variance in the data. PC1 is a linear combination of the original variables. Depending on the original data values and the weights (coefficients) assigned to each variable in this combination, the resulting values can be positive or negative. The ^{40}K content is most influenced by the PC1 component (positively), i.e., cosmogenic differences in the solar nebula and reactions during the trajectory of the meteoroid (but ^{26}Al and Fa as well). The solar and galactic cosmic radiation effects and secondary neutrons from spallation reactions thrive in the Fe-poor samples and thus the neutron-induced isotope. At the same time, PC2 is positively correlated with Fs and Wo, but explains the second-largest portion of the variance in the data. PC2 is orthogonal to PC1 and ensures that PC2 represents a new dimension of variability that is not captured by PC1.

PC3 represents a new third principal component, however, in these studies, it is not statistically significant. It is usually burdened with the largest error and was therefore not considered in this approach. In almost every sample, ^{40}K from both processes is present, i.e., from the dominant activation process (PC1) and nucleosynthesis (PC2). According to Figure 6, ordinary chondrites show the greatest contribution from the PC1 factor and a smaller, negative contribution from the PC2 factor. The negative sign of the variability factor in PC2 case indicates a loss of ^{40}K from the nucleosynthesis process. Ordinary chondrites most likely lost the isotope due to its radioactive decay, or a significant amount of ^{40}K was lost due to other processes during the early stage of CREA exposure. In the case of the lunar meteorite, the dominant factor determining the ^{40}K content is nucleosynthesis, while this meteorite shows a deficiency in ^{40}K content from nuclear reactions. Alternatively, ^{40}K could activate but did not, likely due to material being too deep within the parent body or meteoroid. It is important to note that the efficiency of the activation process will vary with the depth of the material. Activation processes will be weakest deep inside an asteroid, which is why shielding depth in the parent body is so crucial in determining the cosmogenic isotope production, including noble gases as well as ^{40}K. This may be evidence that the Moon formed from material more isolated from cosmic radiation (material from the deeper layers of the forming planet/planets).

Therefore, the PC1 factor reflects the accumulation process of ^{40}K from nuclear reactions, which depends on several important parameters: chemical composition (availability of ^{40}Ca, ^{39}Ar, ^{39}K and iron Fe isotopes), efficiency of the activation process (mainly cross-section), as well as the duration of CREA. In general, the oldest meteorites, which have not undergone other processes conducive to fractional potassium, should exhibit the highest contribution of ^{40}K. For meteorite clans with similar composition and origin, the PC1 component can determine the CREA of meteoroids. This is confirmed by the dominant contribution of the PC1 factor in iron meteorites, mesosiderites, and aubrites.

CONCLUSIONS

This comprehensive overview of potassium ^{40}K in the context of meteoritics and planetary science, as well as nuclear processes, covers multiple aspects of potassium's occurrence, behaviour, and significance. A set of 32 specimens of various meteorites was analysed using a unique low-background gamma spectrometry system. The ^{40}K isotope concentration of the different meteorites vary in a wide range (three orders of magnitude), between 0.5 and 26.2 Bq/kg (21.9 ±0.5 dpm/kg to 2661 ±90 dpm/kg), providing a broader range than previously presented in the literature. The lowest ^{40}K content was recorded in NWA 15015 mesosiderite, while the highest in Chelyabinsk (LL5) ordinary chondrite. Generally, according to our results, we can also see this trend in other samples – the highest content of ^{40}K is found in ordinary chondrites (L and LL) and the lowest in mesosiderite (stony-iron meteorite).

Based on the obtained research results, the authors believe that by analyzing a much larger number of different types of meteorites, it will be possible to obtain significant information about their origin and time of exposure to cosmic radiation. In this aspect, lunar meteorites may constitute an excellent model for meteorites in which ^{40}K is mainly associated with nucleosynthesis, and the role of exposure to cosmic radiation is very limited due to the very short CREA – ranging from only several tens of thousands of years to several million years.

Data Availability Statement: The data underlying this article will be shared on submission of a reasonable request to the corresponding author.

REFERENCES

Albarède F., 2009. *Geochemistry: An Introduction*. Cambridge University Press, Cambridge, UK. https://doi.org/10.1017/CBO9780511807435.

Alexander C.M.O'D., Boss A.P. & Carlson R.W., 2001. The early evolution of the inner solar system: A meteoritic perspective. *Science*, 293(5527), 64–68. https://doi.org/10.1126/science.1052872.

Ammon K., Masarik J. & Leya I., 2009. New model calculations for the production rates of cosmogenic nuclides in iron meteorites. *Meteoritics & Planetary Science*, 44(4), 485–503. https://doi.org/10.1111/j.1945-5100.2009.tb00746.x.

Atwood D.A. (ed.), 2010. *Radionuclides in the Environment*. Wiley, UK.

Barr A.C., 2016. On the origin of Earth's Moon. *Journal of Geophysical Research: Planets*, 121, 1573–1601. https://doi.org/10.1002/2016JE005098.

Bloom H., Lodders K., Chen H., Zhao C., Tian Z., Koefoed P., Pető M.K., Jiang Y. & Wang K., 2020. Potassium isotope compositions of carbonaceous and ordinary chondrites: Implications on the origin of volatile depletion in the early solar system. *Geochimica et Cosmochimica Acta*, 277, 111–131. https://doi.org/10.1016/j.gca.2020.03.018.

Bogard D., Burnett D., Eberhardt P. & Wasserburg G.J., 1967. ^{40}Ar–^{40}K ages of silicate inclusions in iron meteorites. *Earth and Planetary Science Letters*, 3, 275–283. https://doi.org/10.1016/0012-821X(67)90048-9.

Burnett D.S., Lippolt H.J. & Wasserburg G.J., 1966. The relative isotopic abundance of ^{40}K in terrestrial and meteoritic samples. *Journal of Geophysical Research*, 71(4), 1249–1269. https://doi.org/10.1029/JZ071i004p01249.

Ciesla F.J., 2008. Radial transport in the solar nebula: Implications for moderately volatile element depletions in chondritic meteorites. *Meteoritics & Planetary Science*, 43, 639–655. https://doi.org/10.1111/j.1945-5100.2008.tb00675.x.

Clayton D., 2003. *Handbook of Isotope in the Cosmos: Hydrogen to Gallium*. Cambridge University Press, New York.

Curry A., Bonsor A., Lichtenberg T., Shorttle O., 2022. Prevalence of short-lived radioactive isotopes across exoplanetary systems inferred from polluted white dwarfs. *Monthly Notices of the Royal Astronomical Society*, 515(1), 395–406. https://doi.org/10.1093/mnras/stac1709.

Dauphas N., Hopp T. & Nesvorný D., 2024. Bayesian inference on the isotopic building blocks of Mars and Earth. *Icarus*, 408, 115805. https://doi.org/10.1016/j.icarus.2023.115805.

David J.-C., Leya I., 2019. Spallation, cosmic rays, meteorites, and planetology. *Progress in Particle and Nuclear Physics*, 109, 103711. https://doi.org/10.1016/j.ppnp.2019.103711.

Długosz-Lisiecka M., 2016. Comparison of two spectrometric counting modes for fast analysis of selected radionuclides activity. *Journal of Radioanalytical and Nuclear Chemistry*, 309(2), 941–945. https://doi.org/10.1007/s10967-015-4688-y.

Długosz-Lisiecka M., 2017. Application of modern anticoincidence (AC) system in HPGe γ-spectrometry for the detection limit lowering of the radionuclides in air filters. *Journal of Environmental Radioactivity*, 169–170, 104–108. https://doi.org/10.1016/j.jenvrad.2017.01.008.

Długosz-Lisiecka M., 2019. Chemometric methods for source apportionment of 210Pb, 210Bi and 210Po for 10 years of urban air radioactivity monitoring in Łódź city, Poland. *Chemosphere*, 220, 163–168. https://doi.org/10.1016/j.chemosphere.2018.12.042.

Długosz-Lisiecka M., Jakubowski T., Krystek M. & El Mallul A., 2022. Radioactive isotopes as a tool for pairing identification of the HAH 346 – Hammadah al Hamra 346 – ordinary chondrites from two separate find areas. *Minerals*, 12(12), 1553. https://doi.org/10.3390/min12121553.

Erkaev N.V., Scherf M., Herbort O., Lammer H., Odert P., Kubyshkina D., Leitzinger M., Woitke P. & O'Neill C., 2023. Modification of the radioactive heat budget of Earth-like exoplanets by the loss of primordial atmospheres. *Monthly Notices of the Royal Astronomical Society*, 518(3), 3703–3721. https://doi.org/10.1093/mnras/stac3168.

Eugster O., Herzog G.F., Marti K. & Caffee M.W., 2006. Irradiation records, cosmic-ray exposure ages, and transfer times of meteorites. [in:]. Lauretta D.S & McSween H.Y. Jr. (eds.), *Meteorites and the Early Solar System II*, University of Arizona Press, Tucson, 829–851.

EXFOR (IAEA), n.d., *Experimental Nuclear Reaction Data (EXFOR) Database Version of 2018*. https://www-nds.iaea.org/exfor/ [access: 22.02.2022].

Fegley B., Jr, Jacobson N.S., Williams K.B., Plane J.M., Schaefer L. & Lodders K., 2016. Solubility of rock in steam atmospheres of planets. *Astrophysical Journal*, 824(2), 103. https://doi.org/10.3847/0004-637X/824/2/103.

Fischer T., Guo G., Langanke K., Martínez-Pinedo G., Qian Y.-Z. & Wu M.-R., 2024. Neutrinos and nucleosynthesis of elements. *Progress in Particle and Nuclear Physics*, 137, 104107. https://doi.org/10.1016/j.ppnp.2024.104107.

Flynn G.J., Consolmagno G.J., Brown P. & Macke R.J., 2018. Physical properties of the stone meteorites: Implications for the properties of their parent bodies. *Geochemistry*, 78(3), 269–298. https://doi.org/10.1016/j.chemer.2017.04.002.

Frizzell K.R., Ojha L. & Karunatillake S., 2023. Bounding the unknowns of Martian crustal heat flow from a synthesis of regional geochemistry and InSight mission data. *Icarus*, 405, 115700. https://doi.org/10.1016/j.icarus.2023.11570.

Gastis P., Perdikakis G., Dissanayake J., Tsintari P., Sultana I., Brune C.R., Massey T.N., Meisel Z., Voinov A.V., Brandenburg K., Danley T., Giri R., Jones-Alberty Y., Paneru S., Soltesz D. & Subedi S., 2020. Constraining the destruction rate of ^{40}K in stellar nucleosynthesis through the study of the ^{40}Ar(p, n)^{40}K reaction. *Physical Review C*, 101, 055805. https://doi.org/10.1103/PhysRevC.101.055805.

Goriely S. & Martínez Pinedo G., 2015. The production of transuranium elements by the r-process nucleosynthesis. *Nuclear Physics A*, 944, 158–176. https://doi.org/10.1016/j.nuclphysa.2015.07.020.

Hampel W. & Schaeffer O.A., 1979. 26Al in iron meteorites and the constancy of cosmic ray intensity in the past. *Earth and Planetary Science Letters*, 42(3), 348–358. https://doi.org/10.1016/0012-821X(79)90043-8.

Herzog G.F., 2007. Cosmic-ray exposure ages of meteorites. [in:] Holland H.D. & Turekian K.K. (eds.), *Treatise on Geochemistry. Volume 1: Meteorites, Comets, and Planets*, Pergamon, 1–36. https://doi.org/10.1016/B0-08-043751-6/01069-0.

Herzog G.F., Moynier F., Albarède F. & Berezhnoy A.A., 2009. Isotopic and elemental abundances of copper and zinc in lunar samples, Zagami, Pele's hairs, and a terrestrial basalt. *Geochimica et Cosmochimica Acta*, 73(19), 5884–5904. https://doi.org/10.1016/j.gca.2009.05.067.

Hin R.C., Coath C.D., Carter P.J., Nimmo F., Lai Y.J., Pogge von Strandmann P.A.E., Willbold M., Leinhardt Z.M., Walter M.J. & Elliott T., 2017. Magnesium isotope evidence that accretional vapour loss shapes planetary compositions. *Nature*, 549(7673), 511–515. https://doi.org/10.1038/nature23899.

Hrynkiewicz A.Z. (red.), 2001. *Człowiek i promieniowanie jonizujące* [Man and ionizing radiation]. Wydawnictwo Naukowe PWN, Warszawa.

Hu Y., Moynier F., Dai W., Paquet M., Yokoyama T., Abe Y., Aléon J., Alexander C.M.O'D., Amari S., Amelin Y., Bajo K., Bizzarro M., Bouvier A., Carlson R.W., Chaussidon M., Choi B.-G., Dauphas N., Davis A.M., Di Rocco T., Fujiya W., …, Yurimoto H., 2024. Pervasive aqueous alteration in the early Solar System revealed by potassium isotopic variations in Ryugu samples and carbonaceous chondrites. *Icarus*, 409, 115884. https://doi.org/10.1016/j.icarus.2023.115884.

Huang T.-Y., Teng F.-Z., Wang Z.-Z., He Y.-S., Liu Z.-C. & Wu F.-Y., 2023. Potassium isotope fractionation during granitic magmatic differentiation: Mineral-pair perspectives. *Geochimica et Cosmochimica Acta*, 343, 196–211. https://doi.org/10.1016/j.gca.2022.11.006.

Hubbard A., 2016. Generating potassium abundance variations in the Solar Nebula. *Monthly Notices of the Royal Astronomical Society*, 460(2), 1163–1172. https://doi.org/10.1093/mnras/stw1005

Huss G.R., 2004. Implications of isotopic anomalies and presolar grains for the formation of the solar system. *Antarctic Meteorite Research*, 17, 132. https://ui.adsabs.harvard.edu/abs/2004AMR....17..132H/abstract.

Huss G.R., Meshik A.P., Smith J.B. & Hohenberg C.M., 2003. Presolar diamond, silicon carbide, and graphite in carbonaceous chondrites: Implications for thermal processing in the solar nebula. *Geochimica et Cosmochimica Acta*, 67(24), 4823–4848. https://doi.org/10.1016/j.gca.2003.07.019.

Jaumann R., Hiesinger H., Anand M., Crawford I.A., Wagner R., Sohl F., Jolliff B.L., Scholten F., Knapmeyer M., Hoffmann H., Hussmann H., Grott M., Hempel S., Köhler U., Krohn K., Schmitz N., Carpenter J., Wieczorek M., Spohn T., Robinson M.S. & Oberst J., 2012. Geology, geochemistry, and geophysics of the Moon: Status of current understanding. *Planetary and Space Science*, 74, 15–41. https://doi.org/10.1016/j.pss.2012.08.019.

Kato C., Moynier F., Valdes M., Dhaliwal J.K. & Day J.M.D., 2015. Extensive volatile loss during formation and differentiation of the Moon. *Nature Communications*, 6, 7617. https://doi.org/10.1038/ncomms8617.

Korda D., Penttilä A., Klami A. & Kohout T., 2023. Neural network for determining an asteroid mineral composition from reflectance spectra. *Astronomy & Astrophysics*, 669, A101. https://doi.org/10.1051/0004-6361/202243886.

Ku Y. & Jacobsen B., 2020. Potassium isotope anomalies in meteorites inherited from the protosolar molecular cloud. *Science Advances*, 6, eabd0511. https://doi.org/10.1126/sciadv.abd0511.

Kun M., Wang S.B. & Jacobsen S.B., 2016. Potassium isotopic evidence for a high-energy giant impact origin of the Moon. *Nature Letters*, 538, 487–490. https://doi.org/10.1038/nature19341.

Lawson T.V., Pignatari M., Stancliffe R.J., den Hartogh J., Jones S., Fryer C.L., Gibson B.K. & Lugaro M., 2022. Radioactive nuclei in the early Solar System: analysis of the 15 isotopes produced by core-collapse supernovae. *Monthly Notices of the Royal Astronomical Society*, 511(1), 886–902. https://doi.org/10.1093/mnras/stab3684.

Li W., Li S. & Beard B.L., 2019. Geological cycling of potassium and the K isotopic response: Insights from loess and shales. *Acta Geochimica*, 38, 508–516. https://doi.org/10.1007/s11631-019-00345-X.

Lock S.J., Stewart S.T., Petaev M.I., Leinhardt Z., Mace M.T., Jacobsen S.B. & Ćuk M., 2018. The origin of the Moon within a terrestrial synestia. *Journal of Geophysical Research: Planets*, 123, 910–951. https://doi.org/10.1002/2017JE005333.

Lodders K. & Fegley B., 1998. *The Planetary Scientist's Companion*. Oxford University Press, New York.

Lugaro M., Ott U. & Kereszturi Á., 2018. Radioactive nuclei from cosmochronology to habitability. *Progress in Particle and Nuclear Physics*, 102, 1–47. https://doi.org/10.1016/j.ppnp.2018.05.002.

Marshall R.R., 1962. Cosmic radiation and the K^{40}–Ar^{40} "ages" of iron meteorites. *Geochimica et Cosmochimica Acta*, 26(10), 981–992. https://doi.org/10.1016/0016-7037(62)90022-4.

Marshall R.R., 1968. Lead–lead age of the Bondoc meteorite. *Geochimica et Cosmochimica Acta*, 32(9), 1013–1018. https://doi.org/10.1016/0016-7037(68)90065-3.

Mayer C., 2012. *Lunar Sample Compendium*. Astromaterials Research & Exploration Science (ARES), NASA. https://curator.jsc.nasa.gov/lunar/lsc/index.cfm [access 22.02.2022].

MBD Meteoritical Bulletin Database, n.d. https://www.lpi.usra.edu/meteor/ [access: 1.07.2023].

MetBase, n.d. https://metbase.org/ [access: 1.07.2023].

Millero F.J., 2014. Physico-chemical controls on seawater. [in:] Holland H.D. & Turekian K.K. (eds.), *Treatise on Geochemistry. Volume 8: The Oceans and Marine Geochemistry*, 2nd ed., Elsevier Science, Amsterdam, Netherlands, 1–18. https://doi.org/10.1016/B978-0-08-095975-7.00601-X.

Napolitani P, Schmidt K.-H., Botvina A.S., Rejmund F., Tassan-Got L. & Villagrasa C., 2004. High-resolution velocity measurements on fully identified light nuclides produced in ^{56}Fe + hydrogen and ^{56}Fe + titanium systems. *Physical Review. Part C: Nuclear Physics*, 70, 054607. https://doi.org/10.1103/PhysRevC.70.054607 NSR:2004NA36.

NDS Nuclear Data Services (IAEA), n.d. https://www-nds.iaea.org/ [access: 22.02.2022].

Nie N.X., Chen X.-Y., Hopp T., Hu J.Y., Zhang Z.J., Teng F.-Z., Shahar A. & Dauphas N., 2021. Imprint of chondrule formation on the K and Rb isotopic compositions of carbonaceous meteorites. *Science Advances*, 7(49), eabl3929. https://doi.org/10.1126/sciadv.abl3929.

Nie N.X., Chen X.-Y., Zhang Z.J., Hu J.Y., Liu W., Tissot F.L.H., Teng F.-Z., Shahar A. & Dauphas N., 2023a. Rubidium and potassium isotopic variations in chondrites and Mars: Accretion signatures and planetary overprints. *Geochimica et Cosmochimica Acta*, 344, 207–229. https://doi.org/10.1016/j.gca.2023.01.004.

Nie N.X., Wang D., Torrano Z.A., Carlson R.W., Alexander C.M.O'D, Shahar A., 2023b. Meteorites have inherited nucleosynthetic anomalies of potassium-40 produced in supernovae. *Science*, 379(6630), 372–376. https://doi.org/10.1126/science.abn1783.

Otuka N., Dupont E., Semkova V., Pritychenko B., Blokhin A.I., Aikawa M., Babykina S., Bossant M., Chen G., Dunaeva S., Forrest R.A., Fukahori T., Furutachi N., Ganesan S., Ge Z., Gritzay O.O., Herman M., Hlavač S., Katō K., Lalremruata B., …, Zhuang Y., 2014. Towards a more complete and accurate experimental nuclear reaction data library (EXFOR): International collaboration between Nuclear Reaction Data Centres (NRDC). *Nuclear Data Sheets*, 120, 272–276. https://doi.org/10.1016/j.nds.2014.07.065.

Palme H., Lodders K. & Jones A., 2014. Solar system abundances of the elements. [in:] Holland H.D. & Turekian K.K. (eds.), *Treatise on Geochemistry. Volume 2: Planets, Asteriods, Comets and the Solar System*, 2nd ed., Elsevier Science, Amsterdam, Netherlands, 15–36. https://doi.org/10.1016/B978-0-08-095975-7.00118-2.

Paniello R.C., Moynier F., Beck P., Barrat J.-A., Podosek F.A. & Pichat S., 2012. Zinc isotopes in HEDs: Clues to the formation of 4-Vesta, and the unique composition of Pecora Escarpment 82502. *Geochimica et Cosmochimica Acta*, 86, 76–87. https://doi.org/10.1016/j.gca.2012.01.045.

Polański A., 1988. *Podstawy geochemii*. Wydawnictwa Geologiczne, Warszawa.

Povinec P.P., Masarik J., Sýkora I., Kováčik A., Beňo J., Meier M.M.M., Wieler R., Laubenstein M. & Porubčan V., 2015. Cosmogenic nuclides in the Košice meteorite: Experimental investigations and Monte Carlo simulations. *Meteoritics & Planetary Science*, 50, 880–892. https://doi.org/10.1111/maps.12380.

Povinec P.P., Sýkora I., Macke R.J., Tóth J., Kornoš L. & Porubčan V., 2020. Radionuclides in Chassigny and Nakhla meteorites of Mars origin: Implications for their pre-atmospheric sizes and cosmic-ray exposure ages. *Planetary and Space Science*, 186, 104914. https://doi.org/10.1016/j.pss.2020.104914.

Przylibski T.A., Długosz-Lisiecka M., Łuszczek K. & Blutstein K., 2023. Results of statistical analysis of primary components concentrations in bulk chemical composition of ordinary chondrite groups. *Meteoritics & Planetary Science*, 58(9), 1246–1259. https://doi.org/10.1111/maps.14050.

Roland J., Debaille V., Pourkhorsandi H. & Goderis S., 2024. Moderately volatile elemental and isotopic variations in variably shocked equilibrated ordinary chondrites from Antarctica. *Icarus*, 412, 115983. https://doi.org/10.1016/j.icarus.2024.115983.

Rosborough S.A., Oliversen R.J., Mierkiewicz E.J., Sarantos M., Robertson S.D., Kuruppuaratchi D.C., Derr N.J., Gallant M.A. & Roesler F.L., 2019. High-resolution potassium observations of the lunar exosphere. *Geophysical Research Letters*, 46(12), 6964–6971. https://doi.org/10.1029/2019GL083022.

Saunier G., Poitrasson F., Moine B., Gregoire M. & Seddiki A., 2010. Effect of hot desert weathering on the bulk-rock iron isotope composition of L6 and H5 ordinary chondrites. *Meteoritics & Planetary Science*, 45(2), 195–209. https://doi.org/10.1111/j.1945-5100.2010.01017.x.

Steller T., Burkhardt C., Yang C. & Kleine T., 2022. Nucleosynthetic zinc isotope anomalies reveal a dual origin of terrestrial volatiles. *Icarus*, 386, 115171. https://doi.org/10.1016/j.icarus.2022.115171.

Taylor S.R. & McLennan S.M., 2012. [Review of the book *Planetary crusts: Their composition, origin and evolution*, by S.R. Taylor & S.M. McLennan]. *Contemporary Physics, 53*(4), 370–371. https://doi.org/10.1080/00107514.2012.672469.

Tian Z., Chen H., Fegley B., Lodders K., Barrat J.-A., Day J.M.D. & Wang K., 2019. Potassium isotopic compositions of howarditeeucritediogenite meteorites. *Geochimica et Cosmochimica Acta*, 266, 611–632. https://doi.org/10.1016/j.gca.2019.08.012.

Varnam M., Hamilton C.W., Aleinov I., Barnes J.J., 2024. Composition and speciation of volcanic volatiles on the Moon. *Icarus*, 413, 116009. https://doi.org/10.1016/j.icarus.2024.116009.

Vasini A., Matteucci F. & Spitoni E., 2022. Chemical evolution of ^{26}Al and ^{60}Fe in the Milky Way. *Monthly Notices of the Royal Astronomical Society*, 517(3), 4256–4264. https://doi.org/10.1093/mnras/stac2981.

Voshage H., Feldmann H., Braun O., 1983. Investigations of cosmic-ray-produced nuclides in iron meteorites: 5. More data on the nuclides of potassium and noble gases, on exposure ages and meteoroid sizes. *Zeitschrift für Naturforschung*, 38(2), 273–280. https://doi.org/10.1515/zna-1983-0227.

Voskresensky D.N., 2023. Structure formation during phase transitions in strongly interacting matter. *Progress in Particle and Nuclear Physics*, 130, 104030. https://doi.org/10.1016/j.ppnp.2023.104030.

Wang K., Li W., Li S., Tian Z., Koefoed P., Zheng X.-Y., 2021. Geochemistry and cosmochemistry of potassium stable isotopes. *Geochemistry*, 81(3), 125786. https://doi.org/10.1016/j.chemer.2021.125786.

Yin Q., 2005. From dust to planets: The tale told by moderately volatile elements. [in:] Krot A.N., Scott E.R.D. & Reipurth B. (eds.), *Chondrites and the Protoplanetary Disk: Proceedings of a Workshop Held at the Radisson Kaua'i Beach Resort, Kaua'i, Hawai'i, 8–11 November 2004*, ASP Conference Series, 341, Astronomical Society of the Pacific, San Francisco, 632–644.

Zerkin V.V. & Pritychenko B., 2018. The experimental nuclear reaction data (EXFOR): Extended computer database and Web retrieval system. *Nuclear Instruments and Methods in Physics Research Section A: Accelerators, Spectrometers, Detectors and Associated Equipment*, 888, 31–43. https://doi.org/10.1016/j.nima.2018.01.045.

Zhao C., Lodders K., Bloom H., Chen H., Tian Z., Koefoed P., Pető M.K. & Wang K., 2019. Potassium isotopic compositions of enstatite meteorites. *Meteoritics & Planetary Science*, 55(6), 1404–1417. https://doi.org/10.1111/maps.13358.